We are IntechOpen, the world's leading publisher of Open Access books
Built by scientists, for scientists

4,800
Open access books available

122,000
International authors and editors

135M
Downloads

Our authors are among the

154
Countries delivered to

TOP 1%
most cited scientists

12.2%
Contributors from top 500 universities

CLARIVATE ANALYTICS
BOOK CITATION INDEX
INDEXED

WEB OF SCIENCE™

Selection of our books indexed in the Book Citation Index in Web of Science™ Core Collection (BKCI)

Interested in publishing with us?
Contact book.department@intechopen.com

Numbers displayed above are based on latest data collected.
For more information visit www.intechopen.com

Chapter 2

Pulse Rate Control for Low Power and Low Data Rate Ultra Wideband Networks

María Dolores Pérez Guirao

Additional information is available at the end of the chapter

http://dx.doi.org/10.5772/52497

1. Introduction

The growing request for low-to-medium data rate low cost networks is raising the interest in wireless sensor networking. For instance in the field of industrial and logistic applications, in order to improve the processes' efficiency the tight monitoring of goods, tools, and machinery -as to their state and position- is required. In response to this interest, IEEE approved in 2003 the IEEE 802.15.4 standard, this being the first one for low data rate, low complexity, and low power wireless networks.

The market success of wireless sensor networks (WSN) requires inexpensive devices with low power consumption. In order to satisfy this requirement, transmission technology, protocol as well as hardware design must give a common answer. UWB radio, particularly with impulse radio transmission (IR), is especially suitable for the development of WSN. IR-UWB is expected to allow low power, low complexity and low cost implementation as well as centimeter accuracy in ranging. The low complexity and low cost characteristics arise from the essentially baseband nature of the signal transmission. The high ranging accuracy results from the large absolute bandwidth, which must be at least 500 MHz. Indeed, the introduction of ranging functionality in low data rate networks was one of the main reasons for the IEEE 802.15.4a (2007) amendment, which added an IR-UWB physical layer to the original standard.

IEEE 802.15.4a allows for the use of non-coherent receivers, and defines ALOHA[1] as the mandatory medium access control (MAC) protocol. The use of a non-coherent receiver, such as an energy detector, helps to minimise power consumption and reduces implementation complexity. The choice of ALOHA is justified by the potential robustness of IR-UWB to multi-user interference (MUI) and by the low data rate nature of the applications envisioned.

In fact, the design of the MAC layer plays a very important role in order to materialize the benefits of IR-UWB in sensor networks. From a networking perspective, one potential

[1] Random medium access scheme that does not check whether the shared medium is already busy before transmission.

INTECH
open science | open minds

©2013 Pérez Guirao, licensee InTech. This is an open access chapter distributed under the terms of the Creative Commons Attribution License (http://creativecommons.org/licenses/by/3.0), which permits unrestricted use, distribution, and reproduction in any medium, provided the original work is properly cited.

benefit of IR-UWB over narrowband radio technologies is the possibility to allow concurrent transmissions by using different pseudo-random, time hopping codes (THCs) as a multiple access (MA) method. However, TH codes are not perfectly orthogonal, and even if, Multi User Interference (MUI) is still a challenge due to the presence of multipath fading and the asynchronicity between sources. Beyond it, non-coherent receivers are less robust to MUI than coherent receivers; particularly, interference coming from close-by interferers can be very harmful. Thus, and specially if non-coherent receivers are used, additional interference mitigation features at the MAC layer are required.

This work is motivated by the fact that interference management at the MAC layer has not been extensively explored in the context of IR-UWB autonomous networks yet. The chapter is organized as follows. A general introduction into the field of IR-UWB radio technology and its relevant technical fundamentals is given in section 2. Additionally, a short overview into current research activities and basic principles of MAC protocol design for low to medium data rate IR-UWB networks is given. It follows a discussion about the use of game theory as a tool to model and analyse distributed MAC algorithms in wireless networks. The section ends with the description of the investigated scenario and the simulation model.

Section 3 introduces distributed Pulse Rate Control (PRC) as a novel approach for interference mitigation in autonomous IR-UWB networks. PRC enables concurrent transmissions at full power, allowing each source to independently adapt its pulse rate - measured in pulses per second (Pps)- to control the impact of pulse collisions at nearby receivers. This section shows that it is possible to incite autonomous users to decrease their impulsive emissions and thus, prevent network resource break-down. Finally, section 4 summarizes the achievements of the work presented and gives directions for future research.

2. Theoretical background

For the understanding of this chapter it is essential to have a good foundation in IR-UWB technology, as well as a general background knowledge of wireless autonomous networks[2] (AN) and game theory. The purpose of this section is to provide a short overview on these three topics. Furthermore, this section describes the scenario and the simulation model used in the investigations.

2.1. Impulse Radio Ultra Wideband (IR-UWB)

IR-UWB is a form of UWB transmission in which data is transmitted using sequences of extremely short pulses with a duration of less than 1ns and a large pulse repetition period (PRP). Due to the extreme short duration of the pulses, IR-UWB is capable of delivering high data rates in the order of several hundred Mbps, but at the expense of reduced transmission range due to the power restrictions.

Inherent to IR-UWB signaling is a high temporal resolution that enables accurate multipath resolution and ranging capabilities. Other interesting features related to the pulsed nature of IR-UWB are its robustness against fading, as well as its low power, low complexity and low cost implementation possibilities. In this respect, IR-UWB is a key technology for providing wireless networks with joint communication and ranging capabilities.

[2] Wireless autonomous networks can be considered as a special subclass of wireless ad hoc and sensor networks with reinforced self-organizing character

This chapter assumes a generic Time-Hopping IR-UWB (TH-UWB) physical layer as described in [21]. Time is divided into frames of length T_f and each user transmits one pulse of length T_p per frame. Furthermore, by dividing the frames into non-overlapping chips of length T_c, multi-access capability is provided. Each user transmits its pulse in a randomly chosen chip, according to a pseudo-random TH sequence (THS). Data modulation follows a pulse position modulation (PPM) scheme. Thus, the signal emitted by the *k*-th TH-PPM transmitter consists of a sequence of pulse waveforms shifted to different times.

$$s^{(k)}(t) = \sum_{j=-\infty}^{\infty} w_{tr}(t - jT_f{}^{(k)} - c^{(k)}[j]T_c - \eta b^{(k)}_{\lfloor j|N_s \rfloor} - \tau^{(k)}), \quad (1)$$

A typical expression is given in 1, where $w_{tr}(t)$ represents the transmitted pulse waveform and T_f is the average frame time, which is also denoted as the mean pulse repetition period. The inverse of the mean pulse repetition period is referred to as the mean pulse repetition frequency, $T_f = \frac{1}{prf}$. The expression $b^{(k)}_{\lfloor j|N_s \rfloor}$ represents that each data symbol $b^{(k)}$ can be transmitted by N_s identical pulses to enhance the quality of reception. The symbol duration equals then $T_s = N_s T_f$. The TH code value for pulse j is given by $c^{(k)}[j]$. The constant term η represents the time shift step introduced by the PPM modulator. Usually, this shift is much smaller than the one due to the TH code (T_c). The time shift $\tau^{(k)}$ represents the relative delay time between the instants at which user k and a reference user i start their transmission; it can be considered as a realization of a random process determined by the actions of the users.

Figure 1 illustrates some of the mentioned parameters; in the example: $N_s = 1$, $c^{(k)} = (2, 3, 4)$, $b^{(k)} = (1, 1, 0)$.

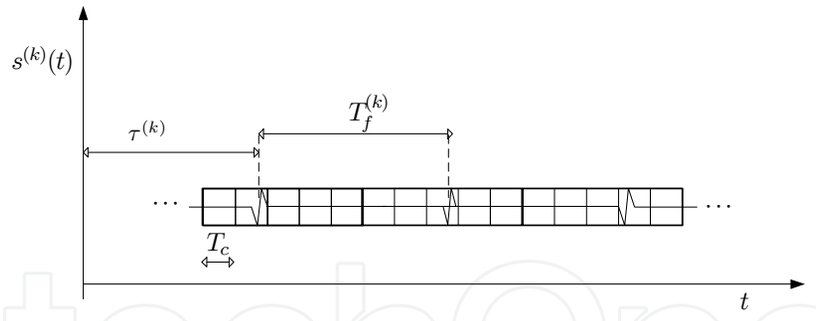

Figure 1. TH-PPM signal structure.

For more detailed information about UWB technology, the author recommends the book [3], which offers an easy-to-read, but complete introduction to the field. Concerning IR-UWB, see [21].

2.2. MAC layer design for low power low data rate IR-UWB networks

The design space for the MAC layer is large; it embraces several dimensions such as multiple access (MA), interference management, resource allocation and power saving. This section summarises the most relevant research findings concerning the design of the MAC layer for low power, low data rate (LDR) IR-UWB networks.

The unique characteristics of the IR-UWB physical layer provide both challenges and opportunities for the MAC layer design. A concrete challenge is the impossibility of carrier sensing, as practised in narrowband systems, since an IR-UWB signal has no carrier. Great opportunities such as robustness against MUI and multipath fading derive from IR-UWB's high temporal resolution. This makes uncoordinated access to the spectrum possible, provided that the local offered load is low compared with the available system bandwidth. For instance, at moderate pulse rates, the "dead time" between pulses allows several uncoordinated, concurrent transmissions to be time interleaved. As a result, ALOHA emerges as the most straightforward MA approach for low data rate IR-UWB networks [3, 9]. The inherent resilience of IR-UWB to MUI can be further increased if different links employ different pseudo-random THC in order to determine the temporal position of the transmitted pulses. The combination of ALOHA with TH coding leads to Time-Hopping Multiple-Access (THMA) [21], which is the most representative MA scheme for low data rate IR-UWB networks.

However TH codes are not perfectly orthogonal, and even if, due to asynchronicity between sources and multipath fading, THMA is still sensitive to impulsive interference. As for CDMA systems, interference coming from a near-by interferer, the so called *near-far* effect, can be very harmful and must be managed in order to avoid performance degradation. For instance, at the physical (PHY) layer multi-user receivers[3] can efficiently address the *near-far* effect at the cost of moderate to high additional hardware [19]. At the link layer, based on the estimation of the wireless link quality, it is possible to adapt the transmission rate to the level of interference experienced at the receiver; the goal can be the improvement of the data rate while satisfying a minimum BER requirement [12].

Within the MAC layer the adaptation of transmission parameters corresponds to a resource allocation task. In the technical literature some approaches on THMA resource allocation can be found, for instance in [18]. A broadly accepted result concerns the optimal power allocation in terms of *proportional fairness*[4]. Note that in autonomous networks with random topology, *proportional fairness* satisfyingly combines fairness and efficiency and outperforms other known performance metrics such as *max-min fairness* or *max total capacity*. This result indicates that the only necessary power control in a IR-UWB network, whose physical layer is in the linear regime[5], is the scheduling function $0 - P_{max}$. In other words, each node should either transmit with full power or not transmit at all [18]. Another common finding is the existence of an *exclusion region* around every destination such that the reference source and nodes within this area cannot transmit simultaneously. This is similar to the IEEE 802.11 CSMA/CA strategy. Certainly, the *exclusion region* vanishes granted that the system has infinite bandwidth ($W \rightarrow \infty$). However, in a practical IR-UWB network the bandwidth is always finite and the size of the *exclusion region* may become a critical issue forcing the MAC designer to concentrate on the scheduling task.

It can be concluded that for IR-UWB networks, and when maximizing rates is the design objective, near-far effects should be tackled by combining scheduling and rate adaptation. Particularly, for low power networks the optimal MAC layer design follows an "all at once" scheduling while it adapts the transmission rates to interference [18].

[3] Those which can receive on M channels concurrently.

[4] The power allocation that maximises the sum of the log of source rates, which is a concave objective function.

[5] When the rate of a link can be approximated by a linear function of the signal-to-interference-and-noise ratio.

2.3. Basics of game theory

Game theory has been applied in the recent past to model complex interactions among radio devices that have possibly conflicting interests. For the designer of wireless communication systems game theory is a powerful tool to analyse and predict the behaviour of distributed algorithms and protocols. Respected reference books are [7]. A short overview focusing on the application of game theory in the field of wireless communications can be found in [5].

A resource allocation problem can be naturally modeled as a game, in which the players are the radio devices willing to transmit or receive data. In general, there is an interest conflict since the players have to cope with a limited transmission resource such as power, bandwitdh or pulse load. In order to resolve this conflict they can make certain decisions (or take certain actions) such as changing their transmission parameters. The most familiar game form is the *strategic* form, which models a single-shot, simultaneous interaction among players. It is worth to mention that "simultaneous" is not used here in its strict temporal meaning. It does not imply that players have to choose their actions at the same point of time, but much more that no player is aware of the choice of any other player prior to making his own decision.

A *strategic* form game $\Gamma \langle \mathbf{N}, \mathbf{A}, \mathbf{u} \rangle$ is defined by the following elements[6]:

- A set of players, $\mathbf{N} = \{1, 2, ..., |N|\}$ with cardinality $|N|$.
- The possible actions that the players can choose. Assume that player i can choose among $|A_i|$ possible actions (strategies). Then, the set of possible actions of player i is $\mathbf{A_i} = \{a_{i,1}, a_{i,2}, ..., a_{i,|A_i|}\}$, and the game's global action space $\mathbf{A}$ is given by the cartesian product of the action set of each player $\mathbf{A} = A_1 \times A_2 \times ... \times A_{|N|}$. If player i chooses strategy $a_i \in \mathbf{A_i}$ in a game move, the action profile chosen by all players is denoted as the vector $\mathbf{a} = (a_1, a_2, ..., a_{|N|}) = (a_i, a_{-i})$, with $\mathbf{a_{-i}} = (a_1, a_2, ..., a_{i-1}, a_{i+1}, a_{|N|})$ representing the strategies of all players except of player i.
- The utility function, which describes the satisfaction level or payoff of player i given a certain action profile $\mathbf{a}$. The vector of utilities is denoted as $\mathbf{u}(\mathbf{a}) = \{u_1(\mathbf{a}), u_2(\mathbf{a}), ..., u_{|N|}(\mathbf{a})\}$.

To model asynchronous, continuous interactions as those which characterise resource allocation problems in AN the *strategic* form game model is however insufficient. The author agrees with the opinion advanced in [14] and considers *asynchronous, myopic, repeated* games as the most appropriate game model to analyse those problems. At this point it has to be stressed that the work in [14] provides a key result for the application of game theory in the analysis and modeling of AN, since it formalises the relation between the AN's *steady states* and the game behaviour characterised by the Nash equilibria (NE). Theorem 4.1 in [14] proofs that the *steady states* of an AN modeled by an *asynchronous, myopic, repeated* game with stage game $\Gamma \langle \mathbf{N}, \mathbf{A}, \mathbf{u} \rangle$, where all players are rational and act autonomously, coincide with the Nash equilibria of the stage game $\Gamma \langle \mathbf{N}, \mathbf{A}, \mathbf{u} \rangle$.

Notice that an NE is a strategy combination $\mathbf{a}^*$, where no player can improve his utility by individually deviating from its strategy. The existence of an NE for a game significantly

[6] We use bold capital letters to denote sets and bold small letters for vectors; for the sake of simplicity we have omitted the superscript T for transposed vectors

depends on the choice of the utility function; specifically on its mathematical properties. The most common existence result for a game's NE is given by the Glicksberg-Fan-Debreu fixed point theorem [7].

2.4. Investigated scenario

This chapter assumes an autonomous sensor, positioning, and identification network (SPIN) as the example system in all investigations. A SPIN is a system characterized by a medium to high node density (up to 2-3 nodes per m^2) in industrial factories or warehouses. Nodes transmit low to medium rate data (up to 1Mbps) combined with position information (position accuracy under 1m) over medium to long distances (typically less than 30 m) to a common receiver.

Concretly, we consider a cluster of up to a hundred IR-UWB sensor nodes that transmit data packets to one common receiver, called the cluster head (CH). The network operation model is based on the beacon-enabled mode of the IEEE 802.15.4a standard [8]. Each sensor node (SN) is considered a source; a link is formed by a transmitting node (source) and the cluster head (CH). Users are asynchronous among themselves. We investigate two scenarios:

- **Scenario 1- Continuous transmission**: Up to 10 UWB sensor nodes are equidistantly situated to the CH, but not necessarily to themselves, along a circle of radius 10 m. They continuously send packets to the CH.
- **Scenario 2- Factory hall**: This scenario accounts for a square simulation field with dimensions 30m$\times$30m. In this field, 100 IR-UWB sensor nodes are considered: 5 are collocated at fixed positions, 75 move along a production line at 5m/s while the rest randomly moves at the same speed within the simulation field. It is assumed that each sensor node generates packets following an exponential distributed packet inter-arrival process and that the exponential processes of the individual sensor nodes are statistically independent. The maximum information data rate per sensor node is 50 Kbps.

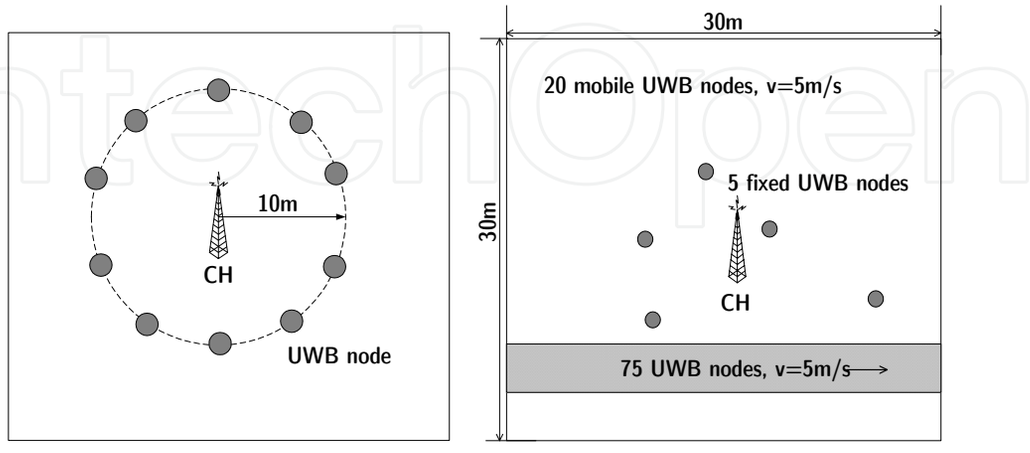

Figure 2. Investigated scenarios: (a) Continuous transmission vs. (b) Factory hall.

2.5. Simulation model

The dynamic simulation model has been developed with the discrete event simulation system OMNeT++ [15]. The CH and each SN comprise a PHY layer, a DLC layer and an application layer instance; network and transport layer operation is transparent. For the air interface the superframe structure described in Section 5.4.1 of the IEEE 802.15.4a standard [8] has been selected.

At the application layer each SN generates data packets according to an exponential distributed packet inter-arrival process. Packets are addressed to the CH; its size has been chosen to be $L_p = 400$ bits. The exponential processes are statistically independent from each other, and a maximum information data rate of 1 Mbps is considered. The DLC layer implementation corresponds with the basic "data transfer model to a coordinator" in the standard IEEE 802.15.4a [see 8, Section 5.5.2.1]. For each DLC packet a packet error rate (PER) is calculated as a function of the received power, interference from concurrent transmissions and thermal noise. At the MAC layer a link adaptation function has been implemented which aims at optimising link/system capacity under several channel and interference conditions. The development and analysis of this function is the main achievement of the work presented in this chapter and is covered in section 3.

It is assumed that the network has a fixed chip duration, T_c, so that all changes at the PHY layer transmission parameters are induced by instructions coming from the MAC/DLC layer. The selected set of PHY layer parameters remains constant for one MAC packet transmission, but can be changed from packet to packet according to the time variant channel and interference conditions.

3. MUI Mitigation by distributed pulse rate control

Interference mitigation is a fundamental problem in wireless networks. In CDMA systems, a well-known technique for this is to control the nodes' transmit powers [22]. The work in [17] has shown that for wireless networks in the *linear regime*, and that allow fine-grained rate adaptation, the optimal power allocation is to let nodes either transmit at full power or do not transmit at all. IR-UWB conforms to both attributes, and thus, according to [17], the MAC layer should concentrate on alternative interference mitigation techniques such as scheduling and rate adaptation.

The term rate adaptation embraces all technical means in a system to adapt the transmission speed (rate) to the current quality of the radio link. In IR-UWB networks, rate control can be achieved by adapting the channel coding rate, the modulation order or the processing gain. In order to adapt these parameters, the link's transmitter must have an estimate of the level of interference at its intended receiver. In autonomous networks, most approaches make use of feedback information from the receiver to the transmitter, for example within ACK packets. This information can take various forms; conventionally, it is a function of the signal-to-noise-plus-interference-ratio (SNIR). However, measuring the SNIR is difficult in practice due to the very low transmit power of UWB signals. Therefore, recent approaches [9] rely on information provided by the channel decoder, namely on BER estimations. This work follows theses approaches and also considers BER instead of SNIR feedbacks.

The processing gain of IR-UWB is twofold: the number of pulses per symbol (N_s) and the average frame duration (T_f). The adaptation of IR-UWB processing gain impacts both rate and average emitted power. Adapting the processing gain in IR-UWB systems was first suggested by Lovelace et. al. in [10]. Lovelace proposed a technique for adjusting the number of pulses per symbol in a single-hop link affected by uncoordinated near pulse interferers. This technique requires a particular type of receiver, capable of selectively and passively blank large interfering pulses from symbol decisions. Also, the approach assumes a system with a large number of pulses per symbols, so that blanking a few of them has only a minimal impact on the resulting BER. The joint adaptation of both types of processing gain was first studied in the context of IEEE 802.15.3a WPANs to reduce the mutual interference among uncoordinated, collocated WPANs [23], and was lately extended to cluster based wireless sensor networks in [20]. The basic observation in [23] was that the larger the number of collocated WPANs the larger the average frame time, T_f, has to be in order to reduce the amount of impulsive interference.

The first, general, theoretical considerations about the performance tradeoff between the two types of IR-UWB processing gain were published by Fishler and Poor in [6]. Fishler and Poor examined this tradeoff as a function of the BER in a system with fixed processing gain over flat-fading and frequency-selective channels. The study concludes that in a coded system transmitting over a flat-fading channel, the BER is independent of the ratio between the two types of processing gain. In contrast, in an uncoded system over a flat-fading channel and in frequency-selective channels there is a trade-off. This trade-off favours systems with a low number of pulses per symbol, as the system BER considerably degrades as the number of pulses per symbol increases. Thus, regarding processing gain adaptation, and assuming that the energy per transmitted pulse is the same for all users, it is preferable to extend the signal's average frame time (reduce the signal's duty cycle) than to increase the number of pulses per symbol. Moreover, using large frame times help to reduce the system complexity since a lower sampling rate can be used.

With the exception of the work in [10], which requires a particular receiver technique, the distributed adaptation of IR-UWB processing gain in autonomous networks has not been addressed in the literature before. The remaining approaches referenced in this section rely on the presence of a coordinator node that implements the adaptation algorithm and instructs other nodes on how to scale their parameters. This work focuses on autonomous networks; although hierarchical structures are not ruled out here, they are not required and therefore adaptation schemes cannot rely on the presence of coordination entities, but must be distributed.

The author claims that in autonomous IR-UWB networks, due to its self-organising and asynchronous character, and due to the monotonically increasing throughput for increasing pulse rates, the system's local pulse load can become so high that bit errors may not be longer tractable with error coding schemes. Based on this assumption, and following previous theoretical considerations on processing gain adaptation, this work develops a novel mechanism -distributed Pulse Rate Control (PRC)- to coordinate the links' pulse rate levels to optimise the overall network performance, measured in terms of total network logarithmic utility (*proportional fairness*), while satisfying a minimum per link BER requirement.

3.1. Distributed pulse rate control

Pulse rate control (PRC) can be realised in form of a link adaptation function whose goal is the improvement of the network throughput while satisfying a minimum per link BER requirement.

While adaptive modulation and channel coding are local decisions to a sender-receiver pair, PRC involves a cooperation among different links since the average[7] probability of pulse collision at the i-th receiver ($P_{coll,i}$) does not depend on its own link's pulse rate, but on the pulse rates of transmitters in its vicinity [20]. Since the collision probability is an indirect measurement of the BER, it can be further assumed that the BER at the i-th receiver, $P_{e,i}$, does not directly depend on its link's pulse rate, but on the pulse rate of the neighbouring links.

In the following we model, analyse and evaluate the distributed PRC approach. We first formulate PRC as a network logarithmic utility maximisation problem with quality of service (QoS) constraints. In order to solve the problem in a distributed manner, PRC is reformulated to a non-cooperative game with pricing. A distributed asynchronous algorithm is proposed which converges to the globally optimal solution of the original problem.

3.1.1. Problem formulation

The objective of the PRC approach is to determine the maximum pulse rate allocation, such that the QoS demands - in terms of BER- of all network links are fulfilled. This goal can be expressed by equation 2.

$$\max_{\mathbf{prf}} \sum_{i=1}^{|\mathbf{N}|} log\left(r_i(\mathbf{prf})\right)$$

$$\text{subject to:} \tag{2}$$

$$P_{e,i}(\mathbf{prf}_{-i}) \leq \beta_i, \forall\, i \in \mathbf{N},$$

$$prf_i \in \mathbf{PRF}_i = [prf_i^{min}, prf_i^{max}], \forall\, i \in \mathbf{N}$$

PRC assumes that each IR-UWB node can autonomously adapt its average pulse repetition frequency, *prf* - that is the inverse of the average frame duration ($prf = \frac{1}{T_f}$). Aditionally, it assumes that the energy per transmitted pulse, E_p^{tx}, is fixed and equal for all users, independent of the modulation scheme, and is chosen so that the IR-UWB node with the highest data rate completely exploits the FCC requirements in terms of EIRP and peak power. Controlling the source's *prf* is equivalent to controlling it's data rate (r) in terms of pulses per second; with fixed E_p^{tx}, it is also equivalent to controlling the source's average transmitted power.

QoS constraints in equation 2 limits the set of feasible pulse rate allocations. Since a higher pulse rate level from one transmitter increases the collision probability -and in turn the BER

[7] The average is taken over the links' asynchronism. In fact, the collision probability between two transmitters, for instance transmitter j and the reference transmitter i, depends on their pulse rates and on the relative delay time between the instants at which both transmitters start their transmissions. This relative delay is a random variable determined by the action of the users; it is represented by the time shift τ_j.

(P_e)- at neighbouring receivers, there may not be any feasible pulse rate allocation to satisfy the requirements of all users.

The logarithmic utility function in equation 2 captures the link's desire for higher data transmission rate. In an IR-UWB network, the raw data rate per link can be controlled by adapting the channel coding rate (R_i), the modulation order (m_i) or the processing gain, that is the number of pulses per symbol (N_s^i) and/or the average frame duration (T_f^i). Equation 3 depicts the dependency of the raw data rate on these parameters.

$$r_i^{raw} = \frac{1}{N_s^i \cdot T_f^i} \cdot R_i \cdot log_2(m_i) \text{ [bit/s]} \tag{3}$$

Following [6], this work focuses on systems with low number of pulses per symbol. For the sake of simplicity and without loss of generality we consider hereafter $N_s^i = 1, \forall\, i \in \mathbf{N}$. The useful (net) data rate per link is given in equation 4.

$$r_i(\mathbf{prf}) = r_i^{raw} \cdot \left(1 - P_{e,i}(\mathbf{prf}_{-i})\right) \text{ [bit/s]} \tag{4}$$

Since the bit error rate, P_e, is a nonlinear, and neither convex nor concave function of the links' pulse rates, the pulse rate optimisation problem is in general a nonlinear optimisation problem. The classical optimisation theory has no effective method for solving the general nonlinear optimisation problem, but several different approaches such as geometric programming (GP). Each of these approaches involves some compromise [1]; for instance, GP is limited to algorithms with a central single point of computation [2]. Game theory represents an alternative to GP and it is used in the next section to model the PRC problem (in equation 2) in a distributed manner.

3.1.2. Pulse rate control game

From the author's point of view, distributed PRC can be interpreted as a resource allocation mechanism that regulates the link's number of transmitted pulses per second. Hence, the framework of non-cooperative game theory can be applied to model and analyse the problem that searches for the network's maximum pulse rate allocation that satisfies a certain set of per-link BER constraints. Next we show how a game theoretical formulation helps to provide the UWB devices with incentives to minimise impulsive emissions when the cumulative system pulse load excesses certain limits, which are determined by some QoS constraints.

In PRC an increase in a link's average *prf* directly and negatively affects the probability of pulse collision, and consequently the BER, of neighbouring links [20]. A game theorist would refer to this fact by saying that there are *negative externalities* in the system. In order to deal with QoS constraints in the presence of negative externalities cooperation among the autonomous users must be enforced. Pricing is one of the most commonly used incentives to regulate selfish user behaviour and establish cooperation. Keeping this in mind, the original logarithmic utility function $u_i(\mathbf{prf}) = log(r_i(\mathbf{prf}))$ in equation 2 is modified by adding a linear pricing function of the link's *prf*. The new utility function is given in equation 5.

$$v_i(\mathbf{prf}) = log(r_i(\mathbf{prf})) - \pi_i(\mathbf{prf}) \cdot prf_i \tag{5}$$

The original logarithmic utility function reflects the level of a user's satisfaction from consuming the resource *prf* (directly related to the transmission data rate). The pricing factor, $\pi_i(\mathbf{prf})$, reflects the cost per unit of resource charged to user i. Hence, the new utility function can be interpreted as if each user i maximises the difference between its old net utility and a payment to other users in the network due to the interference (pulse collisions) it generates.

With the new utility function $v_i(\mathbf{prf})$ a non-cooperative PRC game with pricing, denoted by $\Gamma_{\text{PRC}} = \langle \mathbf{N}, \mathbf{PRF}, \mathbf{v} \rangle$, is developed. For Γ_{PRC} the set of players $\mathbf{N} = \{1, 2, ..., |N|\}$ corresponds with the set of active links (users) in the network, so that the terms "player" and "user" are used as synonym. The vector of utilities corresponds to $\mathbf{v}(\mathbf{prf}) = \{v_1(\mathbf{prf}), v_2(\mathbf{prf}), ..., v_{|N|}(\mathbf{prf})\}$, and the set of actions that players can choose, $\mathbf{PRF} = PRF_1 \times PRF_2 \times ... \times PRF_{|N|}$, is compact and convex.

As described in 2.4 this work considers a network model with a single centralised receiver (CH) and several uncoordinated sources. With a common pricing factor provided by the CH, $\pi_i(\mathbf{prf}) = \pi_j(\mathbf{prf}) = \pi_{CH}(\mathbf{prf})$, $\forall\, i, j \in \mathbf{N}$, each user in the network can be guided by the altruistic goal of maximising the cumulative network throughput at the CH, while keeping their average bit error rate, $P_{e,i}$, as close as possible to a target $\beta_{CH} = \beta_i, \forall\, i \in \mathbf{N}$. In this setting, the pricing term acts as a control parameter employed by the CH to discourage the overuse of the wireless resource *prf* and to keep the interference sustainable. It is expected that the choice of a common pricing factor for all links degenerates the *proportional-fairness* character of the original problem formulation into a *max-min fairness* solution.

Generally, an average cumulative $P_{e,CH} >> \beta_{CH}$ suggests a congestion situation caused by an overload in the local pulse density. In contrast, $P_{e,CH} << \beta_{CH}$ suggests an underload situation in which the local pulse density is below the sustainable load for the given QoS criteria. Accordingly, the CH measures the cumulative bit error rate at each superframe and continuously tracks its deviation from the target value in the variable $\triangle P^s_{e,CH}$

$$\triangle P^s_{e,CH} = \sum_{k \in \mathbf{AL}^s} P_{e,k} - \beta_{CH}, \tag{6}$$

where s represents the superframe index and $\mathbf{AL}^s$ is the set of active links during superframe s. Based on $\triangle P^s_{e,CH}$, the CH computes a congestion cost for superframe $s+1$ and feedbacks it to the UWB nodes in the next beacon frame. The computation rule for the congestion cost is very simple. If there is congestion in the current superframe s, the congestion cost for the next superframe $s+1$ must be increased, in contrast, if there is underload in the current superframe s, the congestion cost for the next superframe $s+1$ can be decreased. The congestion cost represents a common price factor for all players, $\pi_{CH} = \pi_i, \forall\, i \in \mathbf{N}$. The UWB nodes regulate their *prf*, and therewith their data rate, in response to the congestion cost feedback from the CH.

Specifically, the following computation rule is proposed

$$\pi^{s+1}_{CH} = \begin{cases} (1.0 - \delta)\pi^s_{CH} + \mu \pi^s_{CH} \delta, & \triangle P^s_{e,CH} > 0 \\ (1.0 - \delta)\pi^s_{CH} - \frac{\pi^s_{CH}\delta}{\mu}, & \triangle P^s_{e,CH} < (\beta_{CH}\omega |AL|^s) \end{cases}, \tag{7}$$

where μ is a weight factor and δ is the smoothing factor of a weighted exponential-moving-average (EMA) algorithm [4]. In order to improve game convergence a tolerance region for the cluster congestion level has been defined in which no adaptation is done. The tolerance range is defined by $|AL|^s$, the number of active links in superframe s, and a constant $\omega \leq 0$.

3.1.3. Pulse rate control algorithm

In a realistic distributed environment, at the start of a game it is not possible that a player $i \in \mathbf{N}$ has the complete price information (adjacent channel gains, link qualities) that is necessary to discover an NE inmediately. However, the player can make a guess, denoted by its selected action prf_i, regarding its equilibrium average *prf* denoted by prf_i^*. Then, assuming that the actions of the other players, $\mathbf{prf}_{-i}$, and its own price factor, π_i, remain constant while it makes a decision, player i improves its guess by selecting a new action which maximises its utility function. This new guess results in a new approximation to prf_i^*. When the deviations in all players' actions become negligibly small, the game can be assumed to have converged to an NE.

The PRC algorithm implements the adaptive behaviour described above and distributively solves the pulse rate allocation maximisation problem in equation 2.

PRC Algorithm

- **Step 1: Initialisation**

  For each user $i \in \mathbf{N}$ choose some $prf_i(0) \in PRF_i$ and a price factor $\pi_i(0) \geq 0$.
- **Step 2: Price update**

  At each iteration $t \in T_{i,\pi}$, user i updates its price according to equation 7.
- **Step 3: Pulse rate update**

  At each iteration $t \in T_{i,prf}$, user i updates prf_i according to a best response decision rule:

$$prf_i^*(t+1) = \mathrm{BR}_i\left(\mathbf{prf}_{-i}(t)\right) = \left[\frac{1}{\pi_i(t)}\right]_{prf^{min}}^{prf^{max}} \tag{8}$$

  where the notation $[x]_a^b$ means $\max\{a, \min\{b, x\}\}$ and BR_i is the set of best responses of player i to the strategy profile $\mathbf{prf}_{-i}(t)$.

Notice that the price and *prf* adaptations do not need to happen at the same time. The price update instants are determined by the superframe beacon raster, while the *prf* update instants depend on the beacon raster as well as on the source traffic model and can therefore be asynchronous across users.

In the practical implementation of the algorithm, a discretisation of the action space ($\mathbf{PRF}_i$) is unavoidable. The granularity of this discretisation process represents a trade-off for the convergence properties of the algorithm. An infinitely small granularity equals an infinite action space and guarantees that the NE action profile (if there is one) is considered in the search process; however, it increases the computation cost of the algorithm. With an increasing granularity the action space becomes finite, so that the search space for the algorithm shrinks and the computational cost is reduced. A brief discussion about the existence of Nash equilibria in discrete games can be found in [7]. In general it holds that, if the game with continuous action space has a stable equilibrium, the discrete pendant also has an equilibrium.

3.2. Game analysis

In this section, the utility function of Γ_{PRC} is analysed in terms of existence and uniqueness of Nash equilibria. The fact that Γ_{PRC} fits the framework of potential games ([13, 14]) significantly facilitates the analysis.

A potential game is characterised by the existence of a function, denoted as the potential function, $\Phi : A \rightarrow \Re$, such that the change in the utility function of a player when it unilateraly deviates in its strategy ($\triangle u_i$) is reflected in a change in value of the potential function ($\triangle\Phi$). If for all unilateral deviations, $\triangle\Phi = \triangle u_i$ the game is referred to as an *exact* potential game (EPG). If the relationship between the potential function and the utility functions is relaxed so that only sign changes are preserved, $sgn(\triangle\Phi) = sgn(\triangle u_i)$, the game is called an *ordinal* potential game (OPG).

3.2.1. Existence of an equilibrium

In order to prove the existence of an NE for game Γ_{PRC} a definition and a powerful result concerning the identification of ordinal potential games are leveraged. Definition 1, theorem 1 and 2 and their respective proofs can be found in [14].

Definition 1. *Better-Response Equivalence*

A game $\Gamma = \langle \mathbf{N}, \mathbf{A}, \mathbf{v} \rangle$ *is said to be better response equivalent to game* $\tilde{\Gamma} = \langle \mathbf{N}, \mathbf{A}, \tilde{\mathbf{v}} \rangle$*, if* $\forall\, i \in \mathbf{N}$, $a \in \mathbf{A}$, $v_i(a_i, \mathbf{a}_{-i}) > v_i(b_i, \mathbf{a}_{-i}) \Leftrightarrow \tilde{v}_i(a_i, \mathbf{a}_{-i}) > \tilde{v}_i(b_i, \mathbf{a}_{-i})$.

Theorem 1. *Identification of Ordinal Potential Games*

A game $\Gamma = \langle \mathbf{N}, \mathbf{A}, \mathbf{v} \rangle$ *is an ordinal potential game if and only if it is better response equivalent to an exact potential game.*

Theorem 2. *NE of Better-Response Equivalent Games*

If a game $\Gamma = \langle \mathbf{N}, \mathbf{A}, \mathbf{v} \rangle$ *is better response equivalent to game* $\tilde{\Gamma} = \langle \mathbf{N}, \mathbf{A}, \tilde{\mathbf{v}} \rangle$*, then the Nash Equilibria of* Γ*, if any exist, coincide with the Nash equilibria of* $\tilde{\Gamma}$*.*

With these results in mind, game $\tilde{\Gamma}_{PRC} = \langle \mathbf{N}, \mathbf{A}, \tilde{\mathbf{v}} \rangle$ with utility function

$$\tilde{v}_i(\mathbf{prf}) = log(prf_i) - \pi_{CH} prf_i, \tag{9}$$

is introduced. Since $log(xy) = log(x) + log(y)$ and through definition 1, there is a trivial better response equivalence relationship between Γ_{PRC} and $\tilde{\Gamma}_{PRC}$. Hence, from theorem 2 we know that by analysing the set of Nash equilibria of game $\tilde{\Gamma}_{PRC}$ we are at the same time solving for the Nash equilibria of Γ_{PRC}. Next, we prove that $\tilde{\Gamma}_{\text{PRC}}$ is an EPG and, consequently thanks to theorem 1, Γ_{PRC} is an OPG. Further, in [14] we find a powerful result concerning all potential games with a compact action space and a continuous potential function: The existence of at least one NE.

From [14], a sufficient condition for the existence of a potential function in game $\Gamma = \langle \mathbf{N}, \mathbf{A}, \mathbf{u} \rangle$ is

$$\frac{\partial^2 u_i(\mathbf{a})}{\partial a_i \partial a_k} = \frac{\partial^2 u_k(\mathbf{a})}{\partial a_k \partial a_i}, \forall\, i,\, k \in \mathbf{N}, \forall\, \mathbf{a} \in \mathbf{A} \tag{10}$$

In $\tilde{\Gamma}_{\mathrm{PRC}}$ the utility functions are given by:

$$\tilde{v}_i(prf_i, \mathbf{prf}_{-i}) = log(prf_i) - \pi_{CH} prf_i \tag{11}$$

and

$$\tilde{v}_k(prf_k, \mathbf{prf}_{-k}) = log(prf_k) - \pi_{CH} prf_k. \tag{12}$$

In this network settings, users ignore any influence they may have on the price calculated at the CH. Hence, $\frac{\partial \pi_{CH}}{\partial prf_i} = 0 \, \forall \, i \in \mathbf{N}$, and it is easy to prove that

$$\frac{\partial^2 \tilde{v}_i(prf_i, \mathbf{prf}_{-i})}{\partial prf_i \partial prf_k} = \frac{\partial^2 \tilde{v}_k(prf_k, \mathbf{prf}_{-k})}{\partial prf_k \partial prf_i} = 0 \tag{13}$$

Characteristic for an EPG is the existence of a potential function Φ that exactly reflects any unilateral change in the utility of any player, that is $\triangle\Phi(a) = \triangle u_i(a)$. Hence, starting from any arbitrary strategy vector $\mathbf{a}$ any unilaterally player's adaptation that increases its utility $u_i(a)$ identically translates in an increase of the potential function $\Phi(a)$.

The potential function of game $\tilde{\Gamma}_{\mathrm{PRC}}$ is given in equation 14.

$$\tilde{\Phi}_{\mathrm{PRC}}(\mathbf{prf}) = \sum_{i \in N} log(prf_i) - \pi_{CH} \sum_{i \in N} prf_i \tag{14}$$

Based on the potential game definition given in [13], the proof that $\Gamma = \langle \mathbf{N}, \mathbf{A}, \mathbf{u} \rangle$ is an EPG requires that:

$$u_i(a_i, a_{-i}) - v_i(b_i, \mathbf{prf}_{-i}) = \Phi(a_i, a_{-i}) - \Phi(b_i, a_{-i}), \forall \, i \in \mathbf{N}, \forall \, \mathbf{a} \in \mathbf{A} \tag{15}$$

Equation 16 proves condition 15 for $\tilde{\Gamma}_{\mathrm{PRC}}$. Note that all sum terms in the potential function that are independent of user i's strategy are constant and can be grouped in an extra term denoted as c. By the substraction of the potential functions, the term c dissapears leaving the difference of the potential functions identical to the difference of the utility functions.

$$\begin{gathered}
\tilde{v}_i(prf_i, \mathbf{prf}_{-i}) - \tilde{v}_i(prf_i^{'}, \mathbf{prf}_{-i}) = \tilde{\Phi}_{\mathrm{PRC}}(prf_i, \mathbf{prf}_{-i}) - \tilde{\Phi}_{\mathrm{PRC}}(prf_i^{'}, \mathbf{prf}_{-i}) \\
log(prf_i) - \pi_{CH} prf_i - log(prf_i^{'}) + \pi_{CH} prf_i^{'} = \\
log(prf_i) - \pi_{CH} prf_i \\
+ \underbrace{\sum_{j \in N \wedge j \neq i} log(prf_j) - \pi_{CH} \sum_{j \in N \wedge j \neq i} prf_j}_{=c} \\
-log(prf_i^{'}) + \pi_{CH} prf_i^{'} \\
- \underbrace{\sum_{j \in N \wedge j \neq i} log(prf_j) + \pi_{CH} \sum_{j \in N \wedge j \neq i} prf_j}_{=-c} \\
log(prf_i) - \pi_{CH} prf_i - log(prf_i^{'}) + \pi_{CH} prf_i^{'} = \\
log(prf_i) - \pi_{CH} prf_i - log(prf_i^{'}) + \pi_{CH} prf_i^{'} \\
\forall \, i \in \mathbf{N}, \forall \, prf \in \mathbf{PRF}
\end{gathered} \tag{16}$$

Equation 14 is continuous since it is the sum of continuous functions, furthermore the action space of $\tilde{\Gamma}_{\text{PRC}}$ is compact per definition. Hence, equation 16 verifies that (as any other EPG) $\tilde{\Gamma}_{\text{PRC}}$ has at least one NE. Finally, applying theorem 2 it is proven that Γ_{PRC} has at least one NE - in fact the same as $\tilde{\Gamma}_{\text{PRC}}$).

3.2.2. Uniqueness of the equilibrium

From [14], it is known that an EPG following an asynchronous, myopic, best response decision rule converges to a pure strategy NE that maximises the potential function. Furthermore, if the potential function is strictly concave, it has a unique global maximum which is then the unique NE of the EPG. Based on these results the following proposition can be stated.

Proposition 1. *If $\tilde{\Phi}_{PRC}$ in equation 14 is strictly concave, the proposed PRC algorithm will always converge to the unique NE of game $\tilde{\Gamma}_{PRC}$, which in turn, is the unique global maximum of $\tilde{\Phi}_{PRC}$.*

Proof. The PRC algorithm can be interpreted as the players employing asynchronous myopic best response (MBR) updates. Thus, to demonstrate proposition 1 it suffices to prove the strict concavity of $\tilde{\Phi}_{\text{PRC}}$ in equation 14. As explained in [1, Section 3.1.4], this can be verified with the Hessian matrix and the second-order conditions.

For the Hessian matrix in equation 18 the second derivatives of equation 14 are required.

$$H(\tilde{\Phi}) = \begin{pmatrix} \frac{\partial^2 \tilde{\Phi}_{\text{PRC}}}{\partial^2 prf_1} & \cdots & \frac{\partial^2 \tilde{\Phi}_{\text{PRC}}}{\partial prf_1 \partial prf_j} & \cdots & \frac{\partial^2 \tilde{\Phi}_{\text{PRC}}}{\partial prf_1 \partial prf_N} \\ \vdots & \ddots & \vdots & \ddots & \vdots \\ \frac{\partial^2 \tilde{\Phi}_{\text{PRC}}}{\partial prf_N \partial prf_1} & \cdots & \frac{\partial^2 \tilde{\Phi}_{\text{PRC}}}{\partial prf_N \partial prf_j} & \cdots & \frac{\partial^2 \tilde{\Phi}_{\text{PRC}}}{\partial^2 prf_N} \end{pmatrix} \tag{17}$$

$$\frac{\partial^2 \tilde{\Phi}_{\text{PRC}}}{\partial prf_i \partial prf_j} = \begin{cases} -\frac{1}{prf_i^2} & \text{if } i = j \\ 0 & \text{if } i \neq j \end{cases} \tag{18}$$

The matrix is negative definite, $x^T H(\tilde{\Phi}) x < 0$, since all diagonal elements are negative. Hence, the proof is complete. □

Finally, proposition 1 can be reformulated to proposition 2.

Proposition 2. *If $\tilde{\Phi}_{PRC}$ in equation 14 is strictly concave, the proposed PRC algorithm will always converge to the unique NE of game $\tilde{\Gamma}_{PRC}$, which, in turn, is the unique NE of game Γ_{PRC}.*

Proof. The proof of Proposition 2 results from combining the proof of Proposition 1 with Theorem 2. □

3.2.3. Optimality of the equilibrium

So far, there is no general result about the optimality of Nash equilibria in potential games or in any other more general class of games. However by designing the potential game in a way that its potential function complies with the network design function, a quite elegant way to demonstrate NE optimality is possible. In that case, any strategy that maximises the potential function (any NE) maximises as well the network design function.

In this sense, note that the utility function of game Γ_{PRC} in equation 5, combines the network utility function of the original resource allocation problem (cf. to equation 2) with a linear price function. By exploiting the linear space properties of EPGs, the potential function in equation 14 preserves the properties (such as concavity and uniqueness of the global maximisers) of the original network objective function $\sum_1^{|N|} log(r_i(\mathbf{prf}))$. The addition of the linear price term aims at adjusting the unique NE of $\tilde{\Gamma}_{\text{PRC}}$ so that the QoS constraint in the original problem is respected. Hence the NE is optimal from a network design perspective.

3.3. Performance evaluation

Results highlighted in this section have been computed with the simulation model presented in Section 2.5 in the scenarios depicted in Fig. 2. The aim of this section is to demonstrate the regulative character and the interference compensation functionality of the PRC approach. Therefore, its performance under increasing offered system load is compared to the one obtained with the ALOHA MAC protocol without feedback. Note that the IEEE 802.15.4a proposes ALOHA with optional feedback as the standard MAC protocol for IR-UWB physical layers.

Parameter	**Value**	**Parameter**	**Value**
E_p^{tx}	$2 \cdot 10^{-11}$ [Ws]	BW	1.5 [GHz]
$T_{\int rcx}$	$5 \cdot 10^{-9}$ [s]	*prf* granularity	1 [kHz]
prf_i^{max}	1 [MHz]	prf_i^{min}	10 [kHz]
m-PPM	2	β_{CH}	$5 \cdot 10^{-4}$
L_p	400 bit	μ	2
δ	$1 \cdot 10^{-2}$	ω	$2.5 \cdot 10^{-3}$

Table 1. List of main simulation parameters.

3.3.1. Existence of an equilibrium

First a simplified setting with a constant number of players, as usually assumed in game theory, is considered. Then, a more realistic setting where the number of players is a random variable controlled by the traffic distribution is explored. For both settings simulation results[8] confirm the existence of an NE regardless of the algorithm's initialisation parameters.

Constant number of players This setting considers the continuous transmission scenario described in Section 2.4. Recall that in this scenario up to 10 nodes are collocated along a circumference of 10m radius with the CH in the centre. It is assumed that all nodes have always packets to send; this is assured by configuring the source traffic generator to an information data rate of 1Mbps.

Figure 3 confirms the existence of a stable equilibrium in game Γ_{PRC}, and that the PRC algorithm converges to it. Figure 3(a) depicts a symmetric *prf* allocation, which agrees with the analytically predicted NE; the equilibrium *prf* per link is approximately 220 kHz. In fact, a symmetric equilibrium was expected since the congestion cost is the same for each link and

[8] These results were obtained in [11].

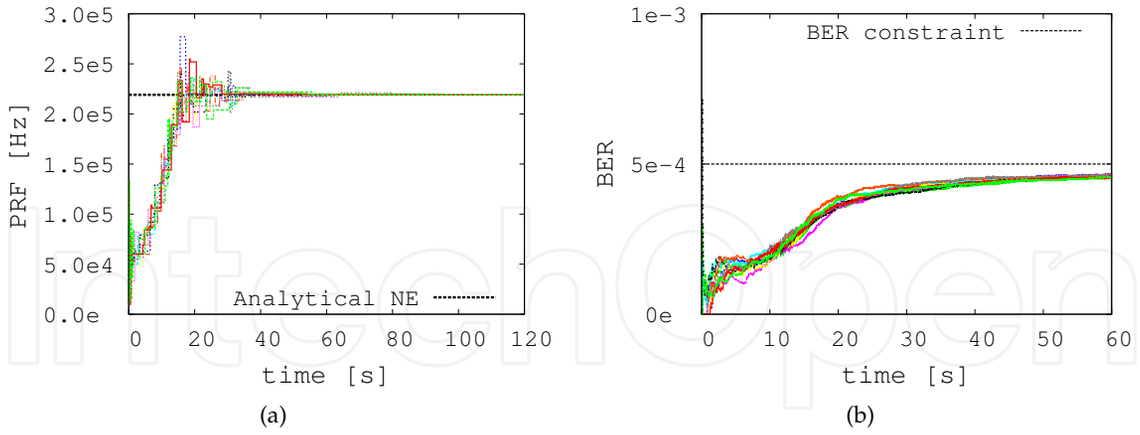

Figure 3. Existence of an equilibrium in Scenario 1 - Continuous transmission. Each link is represented with a different color: (a) Convergence to the unique equilibrium *prf* allocation; (b) Upper-bounded character of the link's BER.

the node topology is symmetric. Figure 3(b) confirms that the QoS constraint on the BER, $P_{e,i} \leq \beta_{CH}$, is fulfilled for all links.

Time-varying number of players This setting considers the factory hall scenario described in Section 2.4. There are a total of 100 heterogeneous nodes, some of them are moving along a production line, others are fixed in known positions and the rest is moving around the CH following a random waypoint movement model. The information data rate has been chosen low enough to guarantee that nodes do not always have packets to send; this results in a time-varying number of players[9].

Figure 4 presents results for two values of the information data rate which are 10 kbit/s and 15 kbit/s, respectively. With 10 kbit/s information data rate, the CH is exposed to a low system pulse load measured in pulses per second (Pps). Figure 4(a) suggests the existence of a stable equilibrium in game Γ_{PRC}, and that the PRC algorithm converges to it. The *prf* equilibrium allocation is again symmetric, with all links converging to the maximum possible *prf* of 1 MHz. Figure 4(b) confirms that the QoS constraint on the BER is satisfied for all links. Note that the BER curves of all links except one follow almost an identical course. The outlier curve corresponds to the sensor node which is located closest to the CH (at 3m) and therefore exhibits the best channel gain and the lowest BER.

By increasing the user data rate to 15 kbit/s, the system pulse load achieves a level which is not compliant with the problem's QoS constraint. The PRC algorithm should then reduce the links' pulse rates to a sustainable level, which is identified by the congestion cost factor π_{CH}. Figure 4(c) illustrates the regulative effect of the PRC algorithm. In spite of the heterogeneous network character, the *prf* equilibrium corresponds to a *max-min* socially fair allocation induced by the choice of a common pricing factor for all links. Besides, it can be observed that in Figure 4(d) some of the links violate the QoS constraint. Still, if we consider the average BER over all links (see Figure 8(b)) it is below the upper bound β_{CH}. This is

[9] Note that the number of players in the game coincide with the number of active links in each superframe, and this is a random variable controlled by the exponential traffic distribution.

due to the global altruistic behaviour of the congestion cost factor, π_{CH}, which works with an estimation of the average[10] BER at each stage of the game.

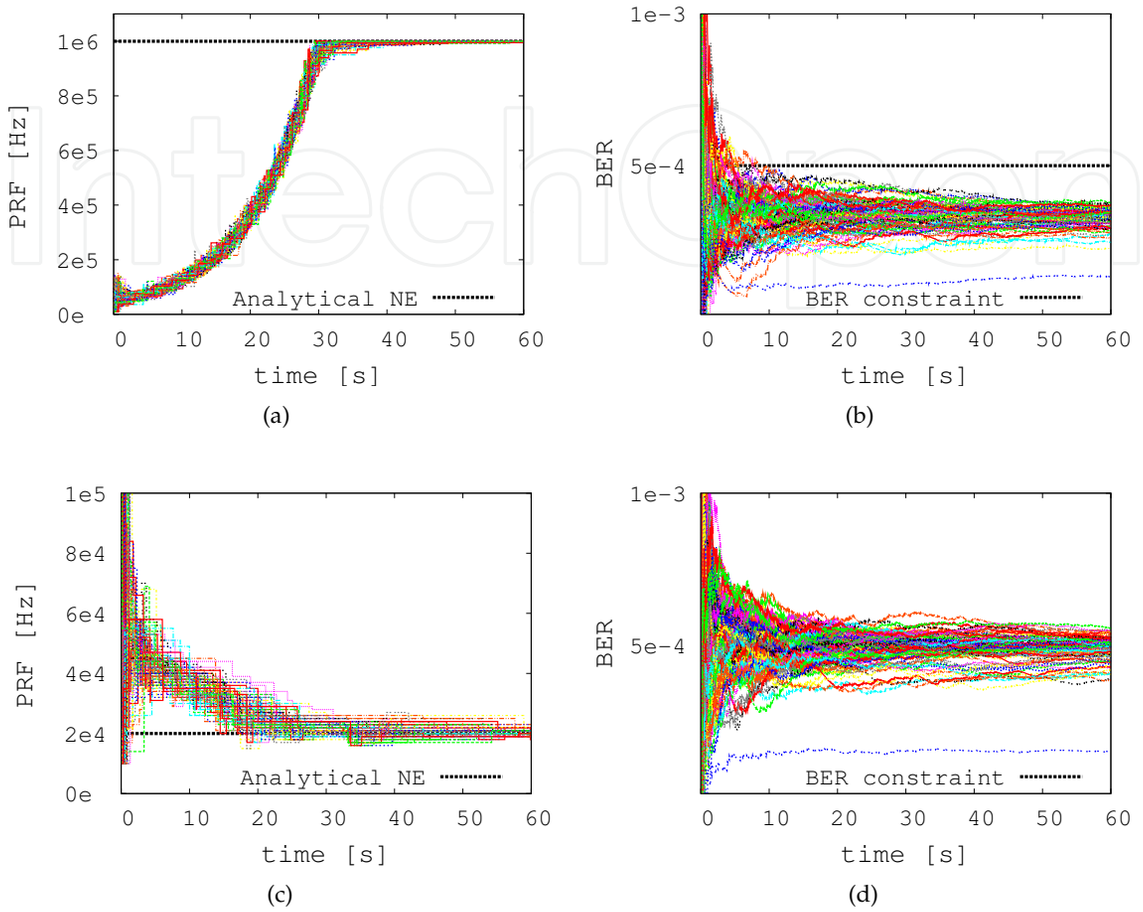

Figure 4. Existence of an equilibrium in Scenario 2 - Factory hall. Each link is represented by a different color: Graphics (a) and (c) show the convergence to the unique equilibrium *prf* allocation when the information data rate per user is 10 kbit/s and 15 kbit/s, respectively; Graphics (b) and (d) show the temporal evolution of the BER per link when the information data rate per user is 10 kbit/s and 15 kbit/s, respectively.

3.3.2. Variation of the offered load

The results in this clause show the effect of increasing offered system load on the aggregate network throughput and the average BER, both measured at the CH. Like in the previous clause, the game performance with a constant number of players is differentiated from the that with a time-varying number of players.

Constant number of players The information data rate is fixed and equal to 1 Mbps to ensure continuous packet transmission. In order to progressively increase the offered system pulse load, the number of sensor nodes collocated along the circumference of 10 m radius has been stepped up from 2 to 10.

[10] Over all links.

In general, and due to the increasing MUI, the aggregated network throughput is expected to drop as the number of nodes in the network grows. Figure 5(a) illustrates the aggregated network throughput. It can be observed that with four to ten source nodes the aggregated network throughput remains almost constant. These results suggest an interference compensation effect of the PRC algorithm; Figure 6 confirms this effect. Additionally, Figure 5(b) shows that the cumulative BER scratches the QoS upper bound in all cases except in the case of having only two nodes. In this special case, even with nodes sending with the maximum *prf* the offered system load is low enough to guarantee an average BER far below the QoS upper bound.

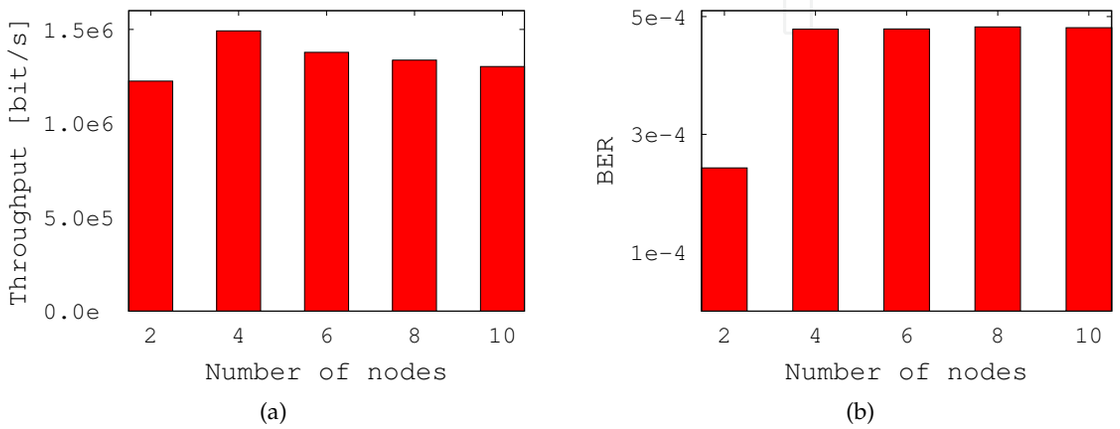

Figure 5. System performance in Scenario 1 - Continuous transmission: (a) Aggregated network throughput measured at the CH's application layer; (b) Average BER per link measured at the CH.

Figure 6 shows the mean[11] *prf* per link; where each link has been represented with a different color. It can be observed that the PRC algorithm relaxes the mean *prf* per link as the number of nodes in the network grows, since consequently the pulse density in the system increases. Recall that a higher pulse density raises the probability of pulse collisions and this, in turn, the probability of bit errors. The larger the average BER at the CH, the larger the congestion factor, π_{CH}, is. Finally, larger congestion factors lead to lower *prf* levels.

Time-varying number of players Since in Scenario 2 - Factory hall the number of sensor nodes is constant, in order to increase the offered system pulse load we progressively raise the information data rate per sensor node.

In Figure 7 two different phases can be identified. As long as the information data rate is kept below 10 kbit/s, the mean *prf* per link does not drop, but remains close to the maximum allowed *prf* value (1 MHz). When the information data rate reaches 15 kbit/s, the mean *prf* per link drops down to approximately 20 kHz and remains there despite growing information data rate. These results are consistent with the PRC algorithm's behaviour illustrated in Figure 4(a) and Figure 4(c).

In a similar way Figure 8 illustrates the regulative behaviour of the PRC algorithm. At information data rates up to 10 kbit/s the PRC algorithm converges to the maximum possible

[11] Over the whole simulation time.

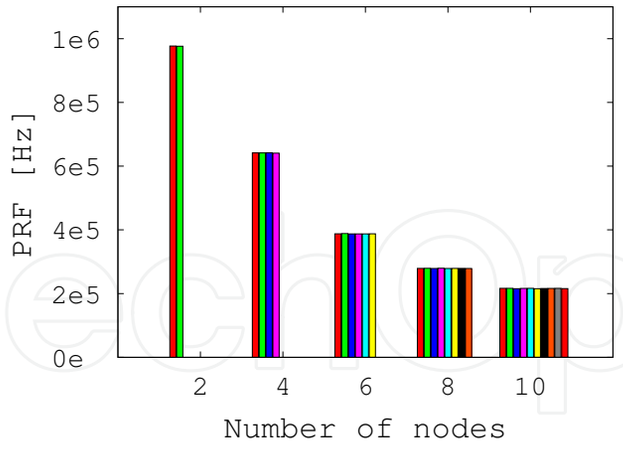

Figure 6. Average *prf* per link in Scenario 1 - Continuous transmission.

prf per link, since the offered system pulse load is low enough to guarantee the QoS constraint on the BER (see Figure 8(b)). With higher information data rates, the PRC algorithm has to relax the effective system pulse load per user to avoid network congestion, and to be able to satisfy the QoS constraint.

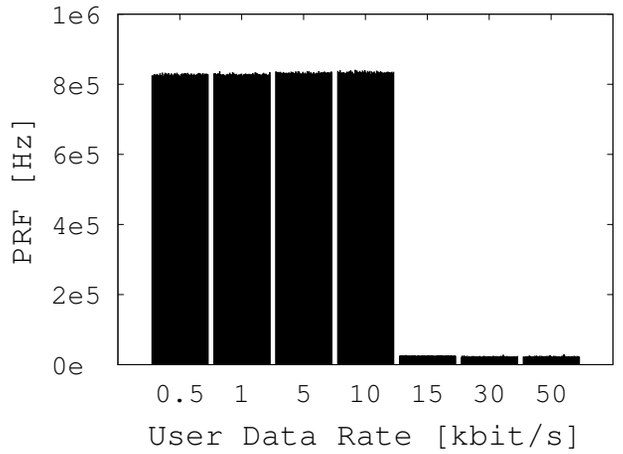

Figure 7. Average *prf* per link in Scenario 2 - Factory hall.

3.3.3. Performance comparison with IEEE 802.14.5a MAC

Finally, this clause is dedicated to compare the performance of the ALOHA MAC protocol, as described in IEEE 802.15.4a, with and without distributed PRC. For the simulations without PRC we have set the fixed *prf* per link to 1 MHz. IEEE 802.15.4a recommends ALOHA with optional feedback channel as the MAC protocol for low data rate sensor networks with IR-UWB physical layers. This work focuses on random access without feedback channel to keep the power consumption and the receiver complexity at the sensor nodes low. In exchange, the drawback has to be accepted that successful reception of data packets cannot be guaranteed since retransmission requests are not possible. Note that in the application field considered in this chapter, the relatively small throughput offered by the random access method without feedback channel is still satisfying.

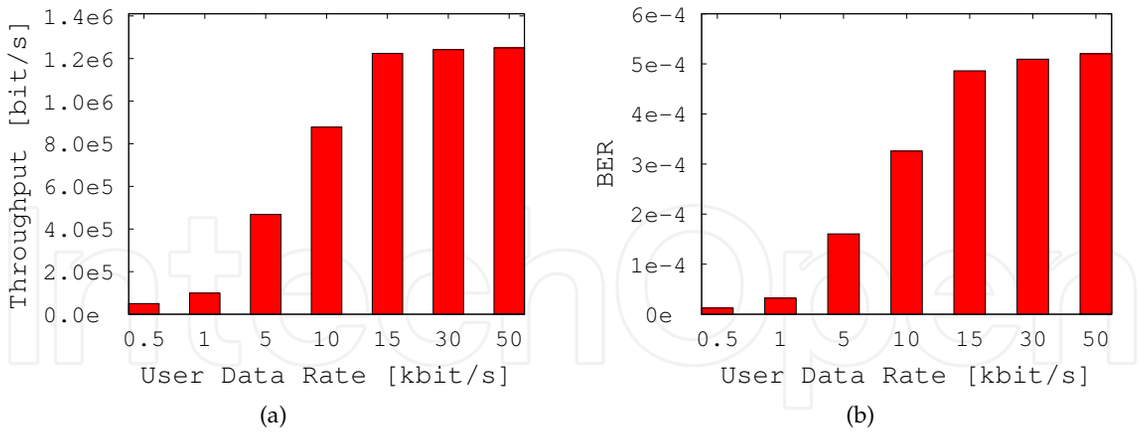

Figure 8. System performance in Scenario 2 - Factory hall: (a) Aggregated network throughput measured at the CH's application layer; (b) Average BER per link measured at the CH.

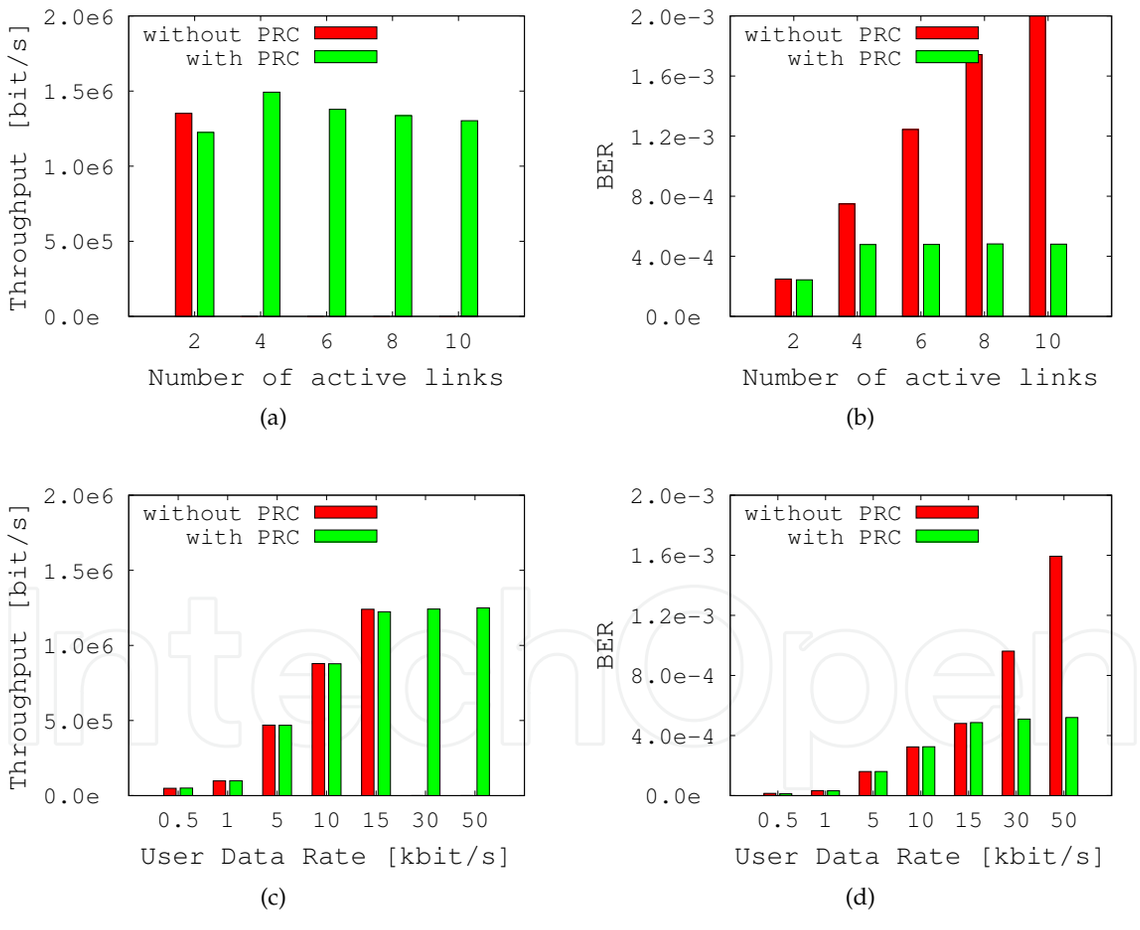

Figure 9. Performance comparison of ALOHA with and without PRC: (a) Aggregated network throughput in Scenario 1; (b) Average BER per link in Scenario 1; (c) Aggregated network throughput in Scenario 2; (d) Average BER per link in Scenario 2.

Figures 9(a) and 9(b) depict a performance comparison between ALOHA with and without PRC in the continuous transmission scenario with high offered pulse load and constant

number of players. The network throughput obtained without PRC rapidly collapses[12] as the number of source nodes grows. This is comprehensible, since pulse collisions (and therewith bit errors, see Figure 9(b)) augment as the offered pulse load increases. In contrast, the interference compensation effect of the PRC approach under increasing offered load can be well observed. Notice how the PRC algorithm is able to limit the system pulse load to a level that ensures the QoS constraint.

Figures 9(c) and 9(d) depict results in the factory hall scenario with low to moderate pulse load and time-varying number of players. Notice that the regulative effect of the PRC approach (see Figure 7) limits the maximum possible cumulative network throughput, while ALOHA with fixed *prf* cannot guarantee the design QoS constraint and breaks down as the information data rate per link increases to 30 kbit/s.

4. Summary and conclusions

This chapter introduces a novel concept for impulsive interference management in low power, autonomous, IR-UWB networks. The concept enables concurrent transmissions at full power, while allowing each source to independently adapt its pulse rate (measured in pulses per second) to reduce the impact of pulse collisions at nearby receivers. The design is independent of a particular modulation scheme and can be applied to any IR-UWB physical layer. Beyond, it does not rely on any particular receiver technique and can work with a simple, low cost, non-coherent receiver.

The chapter formulates and evaluates the pulse rate allocation problem as a social rate optimisation problem with QoS constraints. It introduces a distributed algorithm implementation and analyses its performance via simulation. It has been analytically proven that the game Γ_{PRC} fits the framework of ordinal potential games, and that the NE is unique. In all considered scenarios, simulation results have confirmed the existence of an equilibrium for the game and that the distributed PRC algorithm converges to it, provided that the pricing parameters have been appropriately chosen.

We can conclude that distributed Pulse Rate Control is an appropriate means for impulsive interference management and network throughput optimisation with QoS constraints in highly loaded IR-UWB networks with a common central receiver. In [16] the author extends the work presented here and investigates the applicability of distributed PRC as well as its combination with adaptive channel coding in peer-to-peer networks, i.e. with multiple uncoordinated receivers and without any hierarchical infrastructure. Moreover she investigates a low-complexity, heuristic, alternative algorithm to the one proposed in this chapter that is more suitable for embedded hardware implementations, as preferred in the design of sensor networks.

Acknowledgements

The author thanks Prof. K. Jobmann, Prof. M. G. di Benedetto and Ralf Luebben for their valuable support to complete the work presented in this chapter.

[12] The design QoS constraint can only be guaranteed when the number of active links is below 4.

Author details

Pérez Guirao María Dolores
Institute of Communications Technology (IKT), Leibniz Universitaet Hannover (LUH), Hanover, Germany

5. References

[1] Boyd, S. & Vandenberghe, L. [2006]. *Convex Optimization*, Cambrigde University Press.
[2] Chiang, M., Tan, C. W., Palomar, D., O'Neill, D. & Julian, D. [July 2007]. Power Control by Geometric Programming, *Wireless Communications, IEEE Transactions on* 6(7): 2640–2651.
[3] di Benedetto, M. G. & Giancola, G. [2004]. *Understanding Ultra Wide Band Radio Fundamentals*, Prentice Hall PTR.
[4] Everette, S. & Gardner, J. [October-December 2006]. Exponential Smoothing: The State of the Art–Part II, *International Journal of Forecasting* 22, Issue 4: Pages 637–666.
[5] Felegyhazi, M. & Hubaux, J.-P. [2006]. Game Theory in Wireless Networks: A Tutorial, *Technical report*.
[6] Fishler, E. & Poor, V. [2005]. On the Tradeoff between two Types of Processing Gains, *IEEE Transactions on Communications* 53(9): 1744–1753.
[7] Fudenberg, D. & Tirole, J. [2001]. *Game Theory*, MIT Press.
[8] IEEE *Standard for Information Technology - Telecommunications and information exchange between systems - Local and metropolitan area networks - specific requirement Part 15.4: Wireless Medium Access Control (*MAC*) and Physical Layer (*PHY*) Specifications for Low-Rate Wireless Personal Area Networks (*WPAN*s)* [2007]. *IEEE Std 802.15.4a-2007 (Amendment to IEEE Std 802.15.4-2006)* pp. 1–203.
[9] Le Boudec, J.-Y., Merz, R., Radunovic, B. & Widmer, J. [2004]. DCC-MAC: a Decentralized MAC Protocol for 802.15.4a-like UWB Mobile Ad-Hoc Networks based on Dynamic Channel Coding, *Broadband Networks, 2004. BroadNets 2004. Proceedings. First International Conference on*, pp. 396–405. TY - CONF.
[10] Lovelace, W. & Townsend, J. [16-19 Nov. 2003]. Adaptive Rate Control with Chip Discrimination in UWB Networks, *Ultra Wideband Systems and Technologies, 2003 IEEE Conference on* pp. 195–199.
[11] Luebben, R. [October 2007]. *Spieltheoretische Optimierung des Durchsatzes eines IR-UWB Sensornetzes*, Master's thesis, Institut für Kommunikationstechnik, Leibniz Universität Hannover, Germany.
[12] Merz, R., Widmer, J., Le Boudec, J.-Y. & Radunovic, B. [2005]. A joint PHY-MAC Architecture for Low-Radiated Power TH-UWB Wireless Ad Hoc Networks, *Wireless Communications and Mobile Computing Journal, Special Issue on UWB Communications, John Wiley & Sons Ltd* vol. 5: pp. 567–580.
[13] Monderer, D. & Shapley, S. [1996]. Potential Games, *Games and Economics Behaviour* 14: 124–143.
[14] Neel, J. [2006]. *Analysis and Design of Cognitive Radio Networks and Distributed Radio Resource Management Algorithms*, PhD thesis, Faculty of the Virginia Polytechnic Institute and State University.
[15] *OMNeT++, Discrete Event Simulation System.* [n.d.].
URL: *www.omnetpp.org*

[16] Perez-Guirao, M. [2009]. *Cross-Layer, Cognitive, Cooperative Pulse Rate Control for Autonomous, Low Power, IR-UWB Networks*, Shaker Verlag.
[17] Radunovic, B. & Le Boudec, J.-Y. [13-16 June 2005]. Power Control is Not Required for Wireless Networks in the Linear Regime, *World of Wireless Mobile and Multimedia Networks, 2005. WoWMoM 2005. Sixth IEEE International Symposium on a* pp. 417–427.
[18] Radunovic, B. & Le Boudec, J.-Y. [2004]. Optimal Power Control, Scheduling, and Routing in UWB Networks, *Selected Areas in Communications, IEEE Journal on* 22(7): 1252–1270.
[19] Tong, L., Naware, V. & Venkitasubramaniam, P. [Sept. 2004]. Signal Processing in Random Access, *Signal Processing Magazine, IEEE* 21(5): 29–39.
[20] Weisenhorn, M. & Hirt, W. [Sept. 2005]. Uncoordinated Rate-Division Multiple-Access Scheme for Pulsed UWB Signals, *Vehicular Technology, IEEE Transactions on* 54(5): 1646–1662.
[21] Win, M. & Scholtz, R. [2000]. Ultra-Wide Bandwidth Time-Hopping Spread-Spectrum Impulse Radio for Wireless Multiple-Access Communications, *Communications, IEEE Transactions on* 48(4): 679–689.
[22] Yates, R. [Sep 1995]. A Framework for Uplink Power Control in Cellular Radio Systems, *Selected Areas in Communications, IEEE Journal on* 13(7): 1341–1347.
[23] Yomo, H., Popovski, P., Wijting, C., Kovács, I. Z., Deblauwe, N., Baena, A. F. & Prasad, R. [Sep. 2003]. Medium Access Techniques in Ultra-Wideband Ad Hoc Networks, *in Proc. the 6th Nat. Conf. Society for Electronic, Telecommunication, Automatics, and Informatics (ETAI) of the Republic of Macedonia* .

IntechOpen